Rotational Resonance of Nonaxisymmetric Magnetic Braking in the KSTAR Tokamak

J.-K. Park,[1] Y. M. Jeon,[2] J. E. Menard,[3] W. H. Ko,[2] S. G. Lee,[2] Y. S. Bae,[2] M. Joung,[2] K.-I. You,[2] K.-D. Lee,[2]
N. Logan,[3] K. Kim,[3] J. S. Ko,[2] S. W. Yoon,[2] S. H. Hahn,[2] J. H. Kim,[2] W. C. Kim,[2] Y.-K. Oh,[2] and J.-G. Kwak[2]

[1]*Princeton Plasma Physics Laboratory, Princeton, New Jersey 08543, USA*
[2]*National Fusion Research Institute, Daejeon 305-333, South Korea*
[3]*Princeton Plasma Physics Laboratory, Princeton, New Jersey 08543, USA*
(Received 10 April 2013; published 27 August 2013)

One of the important rotational resonances in nonaxisymmetric neoclassical transport has been
experimentally validated in the KSTAR tokamak by applying highly nonresonant $n = 1$ magnetic
perturbations to rapidly rotating plasmas. These so-called bounce-harmonic resonances are expected to
occur in the presence of magnetic braking perturbations when the toroidal rotation is fast enough to
resonate with periodic parallel motions of trapped particles. The predicted and observed resonant peak
along with the toroidal rotation implies that the toroidal rotation in tokamaks can be controlled naturally in
favorable conditions to stability, using nonaxisymmetric magnetic perturbations.

Control of the toroidal rotation is important in tokamak plasmas since many plasma instabilities, from microscopic to macroscopic scales, can be stabilized by optimizing the toroidal rotation [1–5]. In a next-step device such as ITER [6], the sustainable range of the toroidal rotation becomes narrower since the momentum drives by auxiliary heating are expected insufficient [7], and therefore even more delicate control of the rotation profile would be required in order to access a favorable stability domain in the limited range. One promising tool is magnetic braking [8–10], which is to use nonaxisymmetric magnetic perturbations to induce additional friction forces and toroidal momentum transport. This transport process is well known, and in tokamaks is called neoclassical toroidal viscosity (NTV) transport [8,10–14]. Depending on achievable nonaxisymmetric magnetic configuration, magnetic braking via NTV transport can largely enhance the controllability of the rotation profile.

Understanding of magnetic braking physics has been improved by analytic theories [11,12,15–18] and computations [19–24], and recent dedicated experiments for validation [8,9,13,25]. It is believed that there are two key parameters in NTV transport, collision frequency ν and precession rate, or simply toroidal rotation frequency, ω_p. The effect of the precession becomes important when $\omega_p > \nu/\epsilon$, where $\epsilon = a/R$ is the inverse aspect ratio of tokamak plasmas with the minor radius a and the major radius R, as is expected in high-temperature collisionless plasmas. The fundamental role of precession is the phase mixing of perturbations on the particle trajectories and therefore the suppression of unidirectional transport [24]. There is a mechanism, however, to prevent the phase mixing and to increase the NTV transport even in higher rotation, otherwise the NTV transport will always be smaller by $\propto 1/\omega_p$. This is the so-called bounce-harmonic resonance and this Letter

reports its first experimental validation in the KSTAR tokamak [26].

The bounce-harmonic resonances can occur when the frequencies of the parallel bouncing motion of trapped particles are synchronized with the frequencies of the perpendicular drift motion. That is, $\ell\omega_b \sim n\omega_p$, where ℓ and n are digit numbers, and $\omega_b = 2\pi/\oint dl/v_\parallel$ is the bounce frequency of trapped particles along the field lines l with the parallel velocity $v_\parallel$. In this condition, particle orbit forms a nearly closed loop and the orbit will be subjected to repetitive perturbations if magnetic perturbations are nonaxisymmetric with the toroidal mode n.

In terms of magnetic braking, this implies one can expect strong braking through the rotational resonances when $\omega_p \sim (\ell/n)\omega_b$. The resonant peaks will be placed more often along with the toroidal rotation with higher toroidal n modes, and thus will become more influential on magnetic braking. However, in high n cases, it will be practically difficult to observe the rotational resonances since each resonance is not a very sharp function of rotation as ω_b depends on energy and pitch angle, $v_\parallel/v$, of particles. Obviously $n = 1$ is the best magnetic field perturbation for the test, but $n = 1$ is often strongly coupled to plasma instabilities unless the poloidal field spectrum is highly nonresonant.

Here, the field resonance, which should be distinguished from the rotational resonance, means that the field spectrum of a perturbation is aligned with the helical field lines of the magnetic equilibrium. That is, $m \sim nq$, where m is the poloidal mode number of perturbations and q represents the twist ratio of the field lines in the toroidal direction to the poloidal direction. On the other hand, the highly nonresonant field means the field spectrum is almost orthogonal to the helical field lines, with minimized contents for $m \sim nq$. Such required flexibility for the field spectrum can be almost uniquely found in KSTAR, with
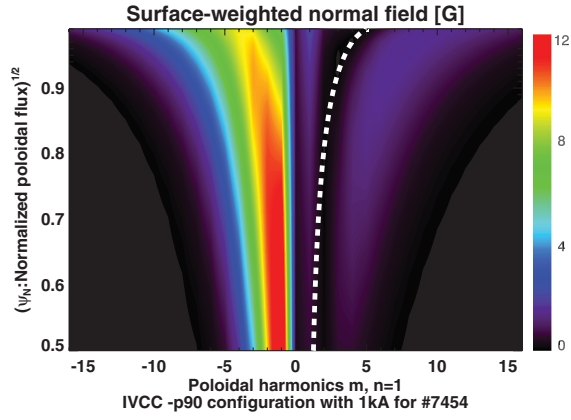
FIG. 1 (color). The spectrum contour of the applied field as a function of poloidal modes m and plasma radius. The white dot line is the locus of the resonant mode $m \sim nq$, and its location on the other side of the spectral peak indicates highly nonresonant characteristics of the applied field.

three rows of in-vessel control coils (IVCC) [27] that covers most of the plasma in the outboard section. This means that a perturbation can be applied in a way of following or crossing the field lines everywhere at the outboard side, and so can be made highly resonant or nonresonant, respectively, by changing the toroidal phase of coil currents between rows. Figure 1 shows the spectrum of the highly nonresonant field used in experiments, as a function of poloidal modes. One can see the spectral peak is located in $m < 0$, while the locus of the resonant spectrum $m \sim nq$ is located on the other side of $m = 0$. The spectrum with the mirror image in $m > 0$ would be highly resonant, as has been actively used for stabilizing edge-localized modes in KSTAR [28]. Note that Fig. 1 includes the field by ideally perturbed plasma currents responding to the applied field, but even the field spectrum merely superposed by the applied field (called vacuum superposition) remains almost the same due to the weak plasma response in this highly nonresonant case.

In the experiments, the highly nonresonant field induced rotational damping without any disturbance to the plasma stability or parameters. Figure 2 shows the time evolutions of important parameters in these discharges. With plasma current $I_P = 600$ kA, the density and temperature were maintained in similar levels, but different levels of rotation were produced by changing input torques and magnetic braking torques. The variation of input torques was to establish different starting points of the rotation before magnetic braking. The neutral beam injection (NBI) was up to ~3 MW but in some cases power was adjusted by modulations at fixed voltage to decrease the rotation. Note in any discharge, NBI blips were required to measure the rotation by charge exchange spectroscopy. The electron cyclotron heating (ECH) in the KSTAR is empirically known to give a countertorque and so was used when the additional rotational reduction was desired. The ECH
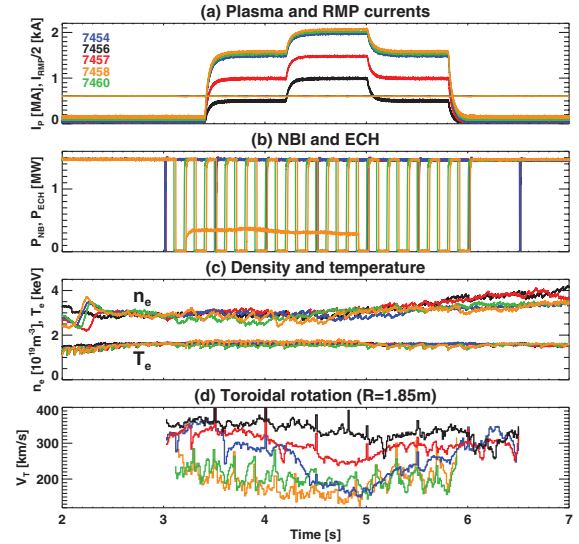

FIG. 2 (color). The time traces of important conditions and parameters in discharges. (a) Plasma currents and two-step pulses of IVCC coil currents, (b) modulated NBI and ECH (green) powers, (c) plasma density and electron temperatures, (d) toroidal rotation measured at the core, where one can see strong rotation braking in a particular level of rotation (blue).

effects on plasma parameters such as temperature were found but not significant (as shown in green in Fig. 2). Then the magnetic braking was applied in two steps, in order to produce two different levels of rotational steady state and to measure braking torques in the different levels.

The results in Fig. 2(d), especially during the upper waveforms at $t = 4.2$–5.0 s, illustrate that the rotational damping increases when the rotation decreases (from black, red, to blue traces), but becomes very small when the rotation is below $V_T \sim 200$ km/s in the core (green and yellow traces). This implies that the rotational damping and torque may have a resonant peak at the particular level of rotation above $V_T \sim 200$ km/s. In fact, without such a rotational resonant peak, NTV theories predict that the rotational damping would keep increasing when the rotation decreases; i.e., $T \propto 1/\omega_p$, which means a rotational equilibrium will be always unstable unless the rotation decreases further and becomes subjected to another regime, where another mechanism begins to dominate the transport process, e.g., superbanana-plateau regime [13].

As noted earlier in this Letter, the possibility of such a rotational resonance has been predicted by theory before and after experiments, as the toroidal rotation in KSTAR is high enough to pass through the well-separated bounce-harmonic resonances when the $n = 1$ magnetic braking is applied. In order to calculate the theoretical torques, the ideal perturbed equilibrium code (IPEC) [29] was used to obtain the nonaxisymmetric variation in the field strength, δB, as shown in Fig. 3. One can see three rows of coils produce the nonresonant field penetrating to the core without significant plasma responses, even if the target plasmas
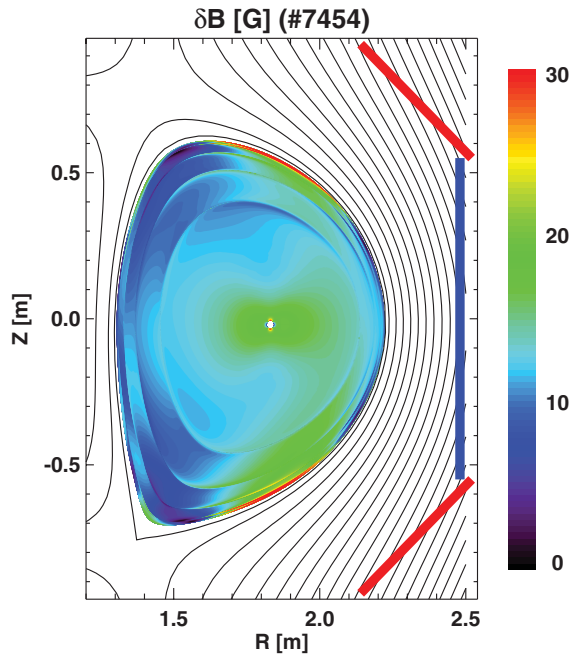
FIG. 3 (color).   The contour of the nonaxisymmetric field variation in the field strength when the $n = 1$ 1 kA in-vessel control coil (IVCC, shown on the right) currents are applied to the KSTAR plasma.

were in high confinement mode (*H* mode) with $\beta_N = 1.9$, where β_N is the plasma pressure divided by the energy density of the toroidal magnetic field, normalized by I_P/aB_{T0}. The resulting nonaxisymmetric field strength is $\delta B/B \sim 10^{-3}$ per 1 kA in IVCC coils in the axisymmetric toroidal field $B_{T0} = 2.0T$ as shown. Then a combined NTV formulation [16] was used to calculate the flux-averaged toroidal torque profiles. Note that the combined NTV calculation uniquely includes bounce-harmonic resonances, although it uses a simple effective collisional operator.

Figure 4 shows the calculated NTV torque as a function of the toroidal rotation in the core, when the highly non-resonant $n = 1$ field is applied with 4 kA IVCC currents. The torque is the volumetric integration of the theoretical NTV torque density in [16] for $0.1 < \psi_N < 0.99$, where ψ_N is the normalized plasma radius in terms of poloidal flux. One can see that each ℓ bounce-harmonic resonance dominates the transport and creates a magnetic braking peak at different levels of the rotation. The higher ℓ has a peak at higher rotation, but their effects become broader and $\ell > 2$ may be difficult to observe. One can see Fig. 4 shows $\ell = 3$ does not exhibit a clear peak in total. Note in this analysis that poloidal rotation was ignored as the toroidal rotation was strong, but its measurement will be important to study the $\ell = 0$ superbanana-plateau regime in lower rotation for the future.

The theoretical calculations based on the IPEC field and a combined NTV formulation predict the $\ell = 1$ bounce-harmonic resonances slightly above $V_T \sim 200$ km/s, as seen in experiments. Actual comparison shows indeed
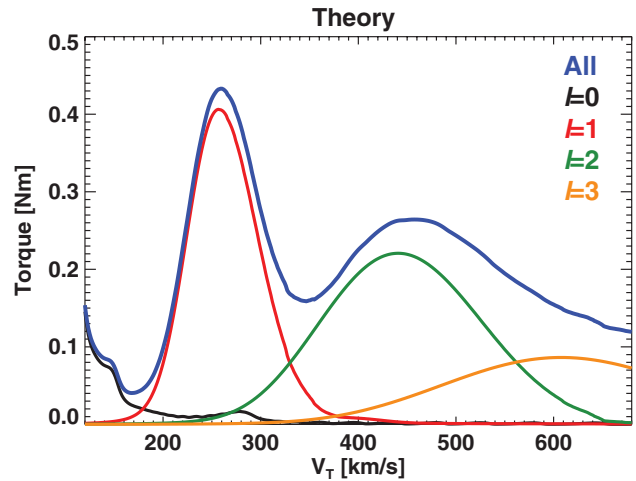

FIG. 4 (color).   The calculated NTV torque as a function of the toroidal rotation in the KSTAR targets when $n = 1$ 4 kA IVCC currents were applied. One can see each bounce-harmonic resonance subsequently dominates the NTV transport.

that the peak positions and values agree between theory and experiment quite well, as shown in Fig. 5. Here the experimental torque is measured by averaging rotational damping rates when the magnetic braking torque is exerted. One assumption that should be noted is the quadratic proportionality of the torque on the variation in the field strength. For instance, the top pulses in Fig. 2 are increased to $I_{IVCC} = 4$ kA from 3 kA, and thus should be scaled by $4^2 - 3^2 = 7$ compared with the case $I_{IVCC} = 1$ kA from 0 kA. The quadratic dependency on δB is fundamental in NTV theory, and has been found robust in numerical simulations [21,23].

The validation of the bounce-harmonic resonances shown in this study has various implications for NTV
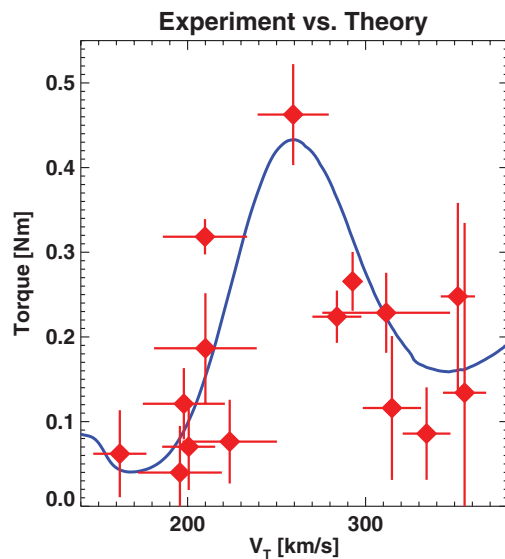

FIG. 5 (color).   The comparison between theory and experiment for the NTV braking torque as a function of the toroidal rotation. Both agree on the resonant rotation and the torque peak values.

transport and magnetic braking in tokamaks. First, NTV transport is enhanced by bounce-harmonic resonances over a wide range of the rotation, especially for higher n applications, as more resonant peaks will exist even in low rotation. It is therefore possible that the high n magnetic braking may induce rotational damping all the way down to the superbanana-plateau regime since NTV transport can become larger and larger through subsequent ℓ resonant peaks when the rotation starts to decrease. The details will depend on the profile variation of the braking torque, and the balance with the injected torque profile, but in general a rotational equilibrium in high rotation can be unstable when a high n perturbation is applied. A lower n, especially $n = 1$, is likely to have a stable point of rotational balance around a well-separated ℓ bounce-harmonic resonance. Once the rotation profile is established nearby such a peak, which is a strong braking point, the equilibrium state can also be kinetically very stable for corresponding $n = 1$ plasma instabilities such as the resistive wall modes [5], as the kinetic energy dissipation is the NTV transport in essence [30]. This implies that nonresonant magnetic braking can be used to automatically find a local stability maxima through the rotational resonances nearby the externally or spontaneously driven rotation, and thus may provide a convenient pathway to optimize the rotation and improve macroscopic stability in ITER and a reactor-scale tokamak.

In summary, magnetic braking experiments in KSTAR have successfully validated the bounce-harmonic resonances in NTV transport, by utilizing the IVCC capability of producing a highly nonresonant $n = 1$ field. The bounce-harmonic resonant peaks were successfully observed, as predicted by theory for the well-separated ℓ peaks and for actual braking torques. This experimental validation implies that the bounce-harmonic resonances are essential to explain NTV torque, especially at high rotation, and can be used to produce a stable rotational balance that will also be kinetically stable.

[1] K. H. Burrell, Phys. Plasmas **4**, 1499 (1997).
[2] S. M. Kaye, R. E. Bell, D. Gates, B. P. LeBlanc, F. M. Levinton, J. E. Menard, D. Mueller, G. Rewoldt, S. A. Sabbagh, W. Wang, and H. Yuh, Phys. Rev. Lett. **98**, 175002 (2007).
[3] E. J. Strait, T. S. Taylor, A. D. Turnbull, J. R. Ferron, L. L. Lao, B. Rice, O. Sauter, S. J. Thompson, and D. Wróblewski, Phys. Rev. Lett. **74**, 2483 (1995).
[4] S. A. Sabbagh, R. E. Bell, J. E. Menard, D. A. Gates, A. C. Sontag, J. M. Bialek, B. P. LeBlanc, F. M. Levinton, K. Tritz, and H. Yuh, Phys. Rev. Lett. **97**, 045004 (2006).
[5] J. W. Berkery, S. A. Sabbagh, R. Betti, B. Hu, R. E. Bell, S. P. Gerhardt, J. Manickam, and K. Tritz, Phys. Rev. Lett. **104**, 035003 (2010).
[6] K. Ikeda, Nucl. Fusion **47**, S1 (2007).
[7] R. V. Bundy, Nucl. Fusion **49**, 085008 (2009).
[8] W. Zhu, S. A. Sabbagh, R. E. Bell, J. M. Bialek, M. G. Bell, B. P. LeBlanc, S. M. Kaye, F. M. Levinton, J. E. Menard, K. C. Shaing, A. C. Sontag, and H. Yuh, Phys. Rev. Lett. **96**, 225002 (2006).
[9] A. M. Garofalo, K. H. Burrell, J. C. DeBoo, J. S. deGrassie, G. L. Jackson, M. Lanctot, H. Reimerdes, M. J. Schaffer, W. M. Solomon, and E. J. Strait, Phys. Rev. Lett. **101**, 195005 (2008).
[10] J.-K. Park, A. H. Boozer, J. E. Menard, A. M. Garofalo, M. J. Schaffer, R. J. Hawryluk, S. M. Kaye, S. P. Gerhardt, S. A. Sabbagh, and NSTX Team, Phys. Plasmas **16**, 056115 (2009).
[11] K. C. Shaing, Phys. Fluids **26**, 3315 (1983).
[12] K. C. Shaing, Phys. Plasmas **10**, 1443 (2003).
[13] A. J. Cole, J. D. Callen, W. M. Solomon, A. M. Garofalo, C. C. Hegna, M. J. Lanctot, H. Reimerdes, and DIII-D Team, Phys. Rev. Lett. **106**, 225002 (2011).
[14] J. D. Callen, Nucl. Fusion **51**, 094026 (2011).
[15] K. C. Shaing, P. Cahyna, M. Becoulet, J.-K. Park, S. A. Sabbagh, and M. S. Chu, Phys. Plasmas **15**, 082506 (2008).
[16] J.-K. Park, A. H. Boozer, and J. E. Menard, Phys. Rev. Lett. **102**, 065002 (2009).
[17] K. C. Shaing, M. S. Chu, and S. A. Sabbagh, Nucl. Fusion **50**, 125012 (2010).
[18] K. C. Shaing, S. A. Sabbagh, and M. S. Chu, Nucl. Fusion **50**, 025022 (2010).
[19] M. Bécoulet, E. Nardon, G. Huysmans, W. Zwingmann, P. Thomas, M. Lipa, R. Moyer, T. Evans, V. Chuyanov, Y. Gribov, A. Polevoi, G. Vayakis, G. Federici, G. Saibene, A. Portone, A. Loarte, C. Doebert, C. Gimblett, J. Hastie, and V. Parail, Nucl. Fusion **48**, 024003 (2008).
[20] Y. Sun, Y. Liang, K. C. Shaing, H. R. Koslowski, C. Wiegmann, and T. Zhang, Phys. Rev. Lett. **105**, 145002 (2010).
[21] S. Satake, H. Sugama, R. Kanno, and J.-K. Park, Plasma Phys. Controlled Fusion **53**, 054018 (2011).
[22] S. Satake, J.-K. Park, H. Sugama, and R. Kanno, Phys. Rev. Lett. **107**, 055001 (2011).
[23] K. Kim, J.-K. Park, G. J. Kramer, and A. H. Boozer, Phys. Plasmas **19**, 082503 (2012).
[24] K. Kim, J.-K. Park, and A. H. Boozer, Phys. Rev. Lett. **110**, 185004 (2013).
[25] Y. Sun, Y. Liang, H. R. Koslowski, S. Jachmich, A. Alfier, O. Asunta, G. Corrigan, C. Giroud, M. P. Gryaznevich, D. Harting, T. Hender, E. Nardon, V. Naulin, V. Parail, T. Tala, C. Wiegmann, S. Wiesen, and JET-EFDA contributors, Plasma Phys. Controlled Fusion **52**, 105007 (2010).
[26] G. S. Lee et al., Nucl. Fusion **40**, 575 (2000).
[27] H. K. Kim, H. L. Yang, G. H. Kim, J.-Y. Kim, H. Jhang, J. S. Bak, and G. S. Lee, Fusion Eng. Des. **84**, 1029 (2009).
[28] Y. M. Jeon, J.-K. Park, S. W. Yoon, W. H. Ko, S. G. Lee, K. D. Lee, G. S. Yun, Y. U. Nam, W. C. Kim, Jong-Gu Kwak, K. S. Lee, H. K. Kim, and H. L. Yang (KSTAR Team), Phys. Rev. Lett. **109**, 035004 (2012).
[29] J.-K. Park, A. H. Boozer, and A. H. Glasser, Phys. Plasmas **14**, 052110 (2007).
[30] J.-K. Park, Phys. Plasmas **18**, 110702 (2011).